# ANALYSIS OF NATURALLY ETCHED SURFACE OF BRASS SHEATHING FROM A NINETEENTH-CENTURY SHIPWRECK

**D. Ashkenazi [a*], A. Inberg [b], and D. Cvikel [c]**

[a] School of Mechanical Engineering, Tel Aviv University, Israel
[b] School of Electrical Engineering, Tel Aviv University, Israel
[c] Leon Recanati Institute for Maritime Studies and Department of Maritime Civilizations,
University of Haifa, Israel

*Abstract*

*The Akko Tower Wreck is ently the remains of a 25-m-long merchant brig, dated to the first half of the nineteenth century. During the 2015 underwater excavation, a piece of brass sheet was retrieved from the shipwreck and its surface and bulk were examined by metallurgical analyses. The examinations revealed a unique example of almost two hundred years' natural etching, which took place in the sea underwater environment. The surface of the sheet was covered with different copper and zinc oxides, which were identified by XRD analysis. Observation of the naturally etched surface with multi-focal light microscopy and SEM-EDS analysis indicated a microstructure of annealed $\alpha$-brass, similar to that of its bulk. S-OES chemical analysis of the bulk revealed a composition of 65.0 wt% Cu, 34.4 wt% Zn and 0.6 wt% Pb. Based on the thickness of the sheet and its good state of preservation, it is suggested that it was used as sheathing to protect the hull against marine organisms, and to improve the sailing qualities of the ship. The results provide further information about the Akko Tower shipwreck; and expand our knowledge regarding the corrosion processes and preservation of brass during a long burial period in marine environments.*

*Keywords: Akko Tower Wreck; Brass sheet; Corrosion; Metallography; Metallurgy; Naturally etched surface*

## 1. Introduction
### 1.1. The Akko Tower Wreck

The historic walled port city of Akko (Acre, St. Jean d'Acre, Akka) is located on a small peninsula which forms the north-eastern extremity of Haifa Bay, in the north of Israel. During the eighteenth and nineteenth centuries, Akko, with its harbour, was considered the key to the East [1], and a factor in land and naval campaigns involving local as well as European armies and navies: from Sidney Smith's blockade during Napoleon Bonaparte's siege in 1799 [2–4], to Muhammad Ali's Egyptian campaign and rule of the town followed by the bombardment of the town by a British-Austrian-Ottoman fleet in 1840 [2, 4, 5]; and the scientific expeditions which called in at the bay of Akko, such as Molyneux, who arrived in the 26-gun sixth-rate frigate HMS *Spartan* in 1847 and launched an expedition to the Dead Sea [6]. During this time, ships of various types, and from various fleets – European, American, and eastern Mediterranean, frequented Akko harbour. From analysis of the archaeological data, it is suggested that the Akko Tower Wreck is the remains of one of these ships.

The Akko Tower Wreck (Fig. 1) was discovered during an underwater survey of the ancient harbour of Akko in 1966. It lies at the entrance to Akko harbour, 35 m north of the Tower of Flies, after which it was named. Since this discovery the shipwreck has been surveyed twice, in 1975 and 1981 [7–9]. However, the researchers came to conflicting conclusions regarding the original ship. Following these, four seasons of underwater excavations were conducted in 2012, 2013, 2015 and 2016 by the Leon Recanati Institute for Maritime Studies of the University of Haifa.

The Akko Tower Wreck was found in 4.4 m of water. The shipwreck remains, oriented north-east to south-west, were 17.8 m between its extremities, and maximum 6.4 m wide. Among the hull remains were sections of the keel, rising wood, keelson, hull planks, framing timbers, ceiling planks, and limber boards. Hull components were made of pine *(Pinus)* and oak *(Quercus)* species. It has been suggested that the original ship was a 25-m-long merchant brig, dated to the first half of the nineteenth century, and built under

the influence of the French shipbuilding tradition [10].

In his report following the 1975 examination of the site, Raban briefly described the exposed wooden components of the shipwreck, and what was identified as zinc sheathing of the hull [8, 9]. According to the quantitative analysis preformed in 1976, the sheathing was composed of 84.38 wt% Zn, 1.95 wt% Pb, 0.06 wt% Fe, and 0.014 wt% Cu [8]. Additional information regarding the type of analysis, other elements, or description of the sheathing, was not presented.

During the 2015 underwater excavation season, a fragment of brass sheet was found at the north-east section of the ship, under the keelson and between framing timbers F73 and F74. The sheet was of irregular shape, perhaps slightly rectangular, with pointed edges, and slightly bent (Fig. 2). It was covered with a brown-green oxide layer, but was well preserved, and in some areas of the sheet a golden-yellow colour was apparent. The sheet was maximum 20.7 cm long and 17 cm wide. Its thickness (including the oxide cover) was measured in five areas and varied between 0.75 mm and 1.07 mm, averaging 0.85 mm.



*Figure 1. General view of the Akko Tower Shipwreck (Photo: A. Yurman)*

Along the longitudinal axis of the sheet are two types of holes, apparently for elliptical and square nails (Figs. 2 and 3). The sheet is slightly folded around the rim of each hole, indicating the direction in which the nails were driven. There are two elliptical holes 7.8 cm apart; one is 9.7×10.7 mm in size, and the other is 9.0×10.2 mm. The square nail holes are spaced at 1–3 cm in two rows: five on the same axis as the elliptical holes, and two close to the surviving edge of the sheet. The square nail sides range between 1.7 mm and 3.7 mm with an average side of 2.9 mm.
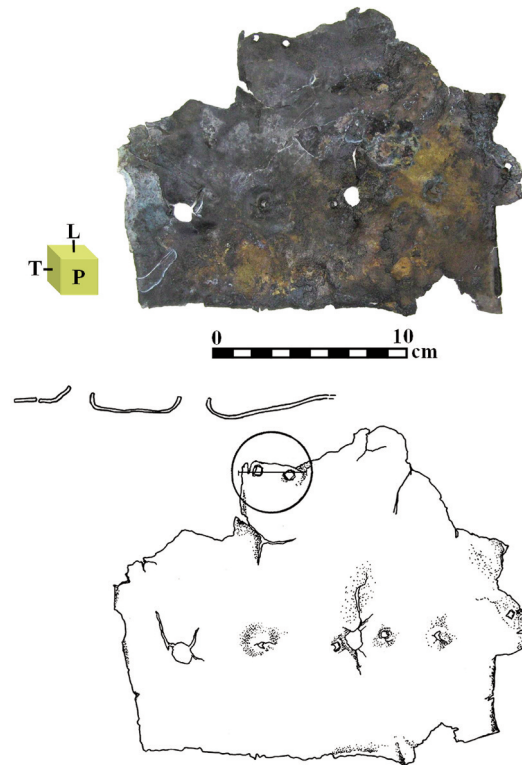


*Figure 2. The as-retrieved brass sheet fragment covered with oxide coating (Photo: D. Cvikel; Drawing: R. Pollak)*



*Figure 3. Multi-focal LM image of the sheet, showing a square hole with deformed boundaries, surrounded by different oxide colours*

### *1.2. Metallographic inspection of ancient metal artefacts retrieved from shipwrecks*

Metallographic examination of ancient metal artefacts retrieved from shipwrecks reveals their microstructure and correspondingly exposes information regarding their manufacturing processes [11–19].

Defining moments in the development of the metallographic scientific field were in 1751, when the geologists Widmanstätten and Schreibers etched various meteorites and exposed their crystalline patterns that could be viewed with a naked eye; and in 1808 when they revealed the well-known Widmanstätten structure by macro-etching [20, 21]. Nevertheless, the English microscopist Sorby, who was the first scientist to observe the microstructure of polished and chemically etched metal samples under the light microscope in 1863, is considered as the founder of metallography [20, 22].

Metallographic etching, which creates contrast in the metallurgical structures of the metal by selective attack of defects, such as different phases and grain boundaries, is considered as an example of controlled selective corrosion process [23]. Vilella was the first scientist who understood the importance of properly grinding and polishing the metal's surface before etching, in order to prevent the observation of false information mostly resulting from depth-of-field limitations [24]. In 1972, Greene and Teterin developed an electrochemical etching technique for improved brass metallographic etching, by determining the appropriate electrolyte, optimum etching potential and time [23].

When ancient metal artefacts retrieved from shipwrecks are examined by metallographic inspection, the metal is commonly cut in longitudinal, planar and transverse cross-sections according to well-known standards, such as the ASTM-E3. Next the metal samples are usually mounted in Bakelite or Epoxy; and the surface is ground with various grades of grit papers and polished with diamond and alumina pastes. Afterward, the polished samples are etched in order to reveal the microstructure of the metal [11–19, 25, 26]. There is a correlation between the composition and microstructure of the retrieved metal and its mechanical properties (such as ductility, hardness, and fracture toughness), as well as to its manufacturing process (e.g., casting, rolling, and annealing). Therefore, examination of the composition, microstructures and properties of ancient brass artefacts retrieved from marine environments may shed light on their manufacturing process; and consequently lead to better understanding of their related materials culture. For example, examination of the brass cases from the Akko 1 shipwreck revealed presence of $\alpha$-brass grains with annealing twins [16, 27]. Such microstructure is typical of brass plate manufactured by rolling and annealing cycles [28, 29].

Today, the most common tools of metallography are the light microscope (LM) and the scanning electron microscope (SEM) [11, 18–20]. However, the use of the advanced 3D digital multi-focal microscope enables non-destructive testing (NDT)

examination of the surface of archaeological artefacts, thus revealing information regarding the topography of the oxide surface and its roughness [30].

### 1.3. Corrosion and conservation of brass artefacts retrieved from shipwrecks

In the last decade the number of studies concerning the corrosion of archaeological bronze and brass objects has increased significantly [30–34]. Brass is extensively used in marine applications because of its mechanical workability, combined with corrosion resistance and good resistance to biofouling due to the high toxicity of cupric ions [35]. However, in some aggressive environments, brass can suffer from zinc dissolution, pitting corrosion and stress corrosion cracking [36]. Since zinc dissolves faster than copper in marine environments, the dezincification process, which accelerates in an acidic chloride solution, leads to an enrichment of copper in the external surface of the brass artefact. The corroded brass surface, attacked by solutions of sodium chloride (NaCl) and ammonium sulphate ($(NH_4)_2SO_4$, during wet-dry cycles, is heterogeneous and composed of different oxides, including $Cu_2O$, $ZnO$ and $Zn_5(OH)_8Cl_2$, which reduces the protective nature of the brass surface [35].

Various oxide layers were observed on the surface of a brass case that was attached to two iron nails, and retrieved from the Akko 1 shipwreck. Observation of the back of the case showed different colours of oxides, including brown-red, greenish-brown, green-yellow, golden-yellowish, pink-reddish, white-grey, greenish and greenish-blue. The oxide colours observed at the surface of the case were explained by the composition of the surface [31]. For example: the reddish colour may be attributed to the presence of cuprite ($Cu_2O$); the pink colour may be due to the presence of zinc hydroxychloride; the white colour was assumed to be related to zinc oxide/hydroxide and/or zinc chloride; the gold-yellowish colour oxide may be attributed to tolbacite ($CuCl_2$); the green colour may have been brochantite, $Cu_4SO_4(OH)_6$, or may have been related to copper chlorides such as atacamite, $Cu_2Cl(OH)_3$; and the blue oxide may be attributed to posnjakite, $Cu_4[(OH)_6SO_4]\cdot H_2O$ [31, 37–39].

The zinc-oxide film provides a passive layer, protecting the brass. However, when the film is damaged the corrosion rate accelerates [35]. Although brass is toxic to many marine organisms, biological activity in the sea environment affects the pH of the water, and therefore plays a significant role in determining the kind of phases formed during the corrosion process [40]. Understanding the corrosion processes and products of archaeological objects is an important step for proper selection of their cleaning,

stabilization and conservation treatments. Moreover, such data may also support information on their authenticity, as well as their dating and origin [41, 42]. Therefore, understanding corrosion processes of brass during long burial periods in seawater is essential.

The brass sheet fragment is the focus of the present article, as part of an ongoing series of studies of the shipwreck and its finds [e.g., 9, 11]. Establishing and comparing the chemical composition, microstructure and properties of this sheet provided information on its manufacturing process and its use in the ship. Thus new information regarding the Akko Tower Wreck was obtained, as well as adding to the existing database related to brass artefacts from other shipwrecks of the period.

## 2. Experimental methods and testing

In order to examine the surface of the brass sheet and to compare it to the bulk of the metal, both non-destructive and destructive metallurgical analyses were performed to the sheet shortly after it was retrieved without applying any stabilization treatment. The following methods were applied (Table 1): visual testing (VT), X-ray fluorescence (XRF) chemical analyses of the oxides at the surface and of the bulk, X-ray diffraction (XRD) for phase identification [31, 43], light microscopy (LM), multi-focal LM and scanning electron microscopy (SEM) including energy dispersive spectroscopy (EDS), metallographic LM observation, and spark optical emission spectroscopy (S-OES) chemical composition of the metal bulk.

The details of the analyses used in this study are:

(a) VT detects visible details, including observed macroscopic defects that may hint at the condition of preservation, the manufacturing process and the use of the sheet.

(b) Hand-held XRF (HH-XRF), for surface chemical analysis before and after grinding the surface (30 seconds for each measurement), using an Oxford X-MET8000 instrument with a silicon drift detector (SDD) equipped with a 45 kV Rh target X-ray tube, with detected area of 5 mm in diameter. The instrument was first calibrated with certificated copper calibration standard sample. Since HH-XRF is a surface analysis tool, in the case of metal artefacts buried underwater, the external surface may not be representative of the object's bulk composition [44]. Hence, the sheet was also examined after grinding its surface to remove the oxide layer and expose the base metal.

(c) XRD patterns of the as-retrieved brass sheet surface for phase identification were obtained on a TTRAX III (Rigaku) $\theta$-$\theta$ diffractometer (equipped with a rotating Cu anode operating at 50 kV and 200 mA). A bent graphite monochromator and a scintillation detector were aligned in the diffracted beam. Two reflection modes were applied: (1) $\theta/2\theta$ scans were performed under specular conditions in the Bragg-Brentano mode with variable slits; and (2) asymmetric $2\theta$ scans with fixed incident angles (at 2º and 3º) were performed with parallel beam optics formed by a multi-layered mirror. It should be noted that the smaller incident angle causes the higher diffraction intensity from the top layers with respect to that from the substrate. Comparison of the patterns exposes the sheet's surface contamination. Phase analysis was performed using the PDF-4+ 2015 database (ICDD) and Jade 9.5 software (Materials Data, Inc.).

(d) A multi-focal and 3D digital LM (HIROX RH-2000) with high intensity LED lighting, including an improved light sensitivity sensor, combining different levels of light intensity and integrated stepping motor, and powerful 3D software with surface topography and roughness measurements.

(e) SEM-EDS analysis was conducted using Environmental SEM (FEI Quanta 200FEG ESEM). The sheet was characterized in high vacuum mode with secondary electron (SE) detector. The composition was analysed by EDS using an Si(Li) liquid cooled X-ray detector calibrated with standard samples, and provided measurements with a first approximation error of 1 %. The scanned area of the different EDS measurements varied between 100×100 µm to 500×500 µm. The Cu/Zn ratio was obtained by omitting other elements than Cu and Zn directly from the EDS's instrument program.

(f) Metallographic examination according to ASTM-E3 Standard; the notation used was P-CS for planar and T-CS for transverse cross-sections. Sample preparation included: (1) 10×10 mm$^2$ sample (P-CS) was cleaned with ethanol, dried and then examined; (2) 10×10 mm sample (P-CS) was cleaned with ethanol and dried, and then chemically polished with $H_3PO_4 \cdot HNO_3 \cdot CH_3COOH$ (11:4:3 ratio) solution; and (3) the samples (P-CS and T-CS) were mounted in Bakelite, ground with silicon carbide papers (240–4000 grits), and then polished with alumina pastes (up to 0.3 µm). The samples were cleaned, and etched with hydrochloric acid in ferric chloride solution ($FeCl_3/HCl/H_2O$).

(g) S-OES analysis was performed with

*Table 1. Surface and bulk analyses preformed on the sheet*

| Analysis | VT | Multi-focal LM | Metallography | XRF | XRD | SEM/EDS | S-OES |
|---|---|---|---|---|---|---|---|
| Surface analysis | + | + | − | + | + | + | − |
| Bulk analysis | + | − | + | + | − | + | + |

Spectrolab (Lab LAVMMC11A Ark/spark machine) in order to examine the chemical composition of the bulk metal. The instrument, which has detection limit < 0.1%, was calibrated with certified leaded brass standard disk before and after the analysis of the brass sheet sample. The examined area was 10×10×0.85 mm, and the surface of the sample was ground and cleaned prior to this test, as recommended in the literature [45].

### 3. Results
#### *3.1. Characterization of the sheet's naturally etched surface*

VT and multi-focal LM NDT observation of the sheet surface revealed holes with deformed boundaries (Figs. 2, 3 and 4). The sheet was covered with heterogeneous layers of oxide, mostly brown to dark green, with some areas yellow-golden, blue, white and pink (Figs. 3 and 4). The LM observation also revealed naturally etched metal with equiaxed $\alpha$ grains (Fig. 4). The oxide layers thickness (T-CS) was measured by LM (after mechanical grinding, polishing and etching), and was 10–150 µm.
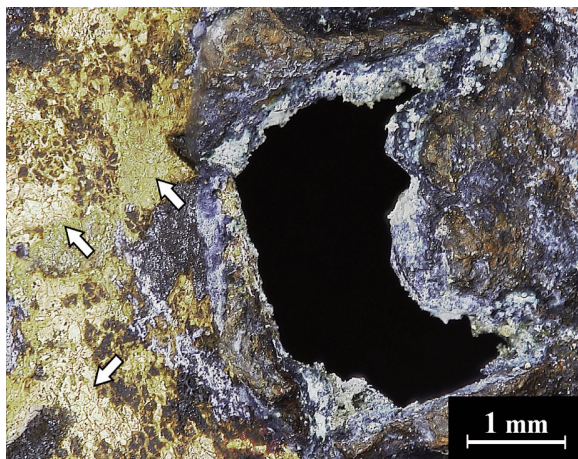


***Figure 4.*** *Multi-focal LM image of the sheet showing a hole with deformed boundaries, surrounded by different oxides and areas of naturally etched metal with equiaxed $\alpha$ grains (left side of the image, arrows)*

HH-XRF NDT examination of the oxide surface (average of eight different areas measured from both sides of the sheet) confirmed that it was originally made of brass, with an average composition of 57.3±4.0 wt% Cu, 39.9±2.9 wt% Zn, as well as the presence of Pb, Si, S and Al (P-section, Table 2). Light elements, such as oxygen and carbon, could not be detected with the present XRF due to instrumental limitations.

The XRD destructive analysis of the sheet surface revealed presence of metallic brass, as well as the presence of different oxides, including cuprite, $Cu_2O$; namuwite, $(Zn,Cu)_4(SO_4)(OH)_6 \cdot 4H_2O$; connellite, $Cu_{19}Cl_4(SO_4)(OH)_{32} \cdot 3H_2O$; and hydrated zinc chloro-sulphate, $Zn_{12}(SO_4)Cl_3(OH)_{15} \cdot 5H_2O$ (Fig. 5).

***Table 2.*** *HH-XRF analysis results of the sheet's oxide surface as-retrieved (average value of eighth measurements) and of the sheet's bulk after grinding (average value of eighth measurements)*

| Description | | As-retrieved oxide surface | Bulk metal |
|---|---|---|---|
| **Composition weight percentage (wt%)** | **Cu** | 57.0±4.0 | 64.7±0.7 |
| | **Zn** | 39.9±2.9 | 34.4±0.4 |
| | **Pb** | 0.4±0.1 | 0.4±0.1 |
| | **Si** | 0.4±0.1 | 0.3±0.2 |
| | **Sn** | – | 0.1±0.1 |
| | **S** | 2.2±1.7 | – |
| | **Al** | 0.1±0.1 | 0.1±0.1 |
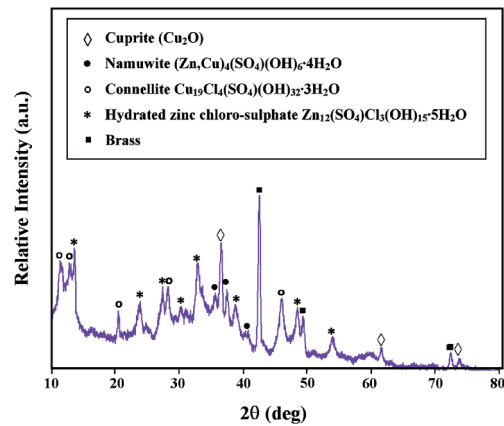


***Figure 5.*** *XRD results of the as-retrieved sheet's oxide surface*
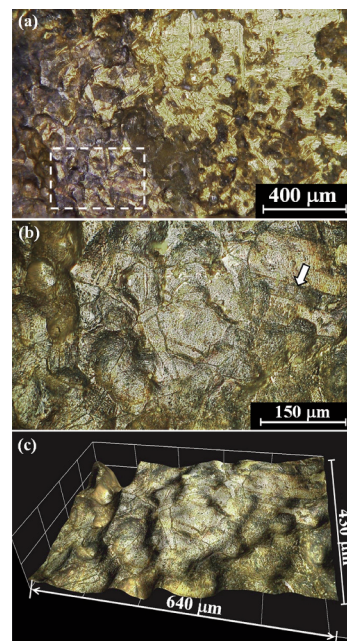


***Figure 6.*** *LM images of the as-retrieved sheet (P-section), showing: (a) general view; (b) equiaxed $\alpha$ grains and some annealing twins (white arrow); and (c) 3D image of the roughness of the naturally etched sheet's surface*

LM image observation of the sheet revealed that it was naturally etched during the long burial period in sea water, with presence of equiaxed α grains and annealing twins (Fig. 6). 3D imaging of the naturally etched sheet exposed the rough surface of the α-brass grains (Fig. 6c).

SEM observation of the as-retrieved sheet (with no further laboratory treatment) revealed α-brass grains with annealing twins (Fig. 7). A similar microstructure
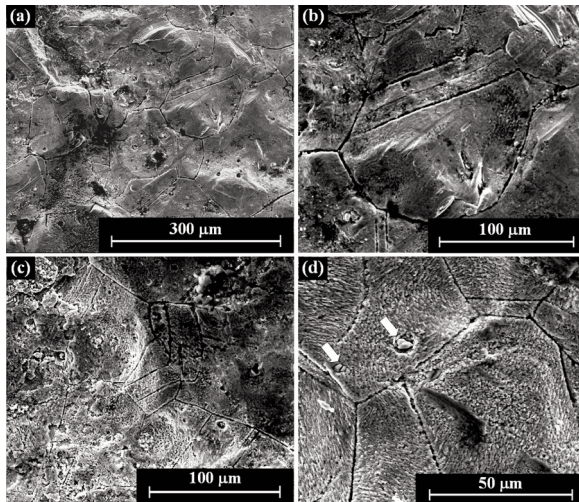


*Figure 7. SEM images of the natural etched sheet (SE mode, P-section): (a) general view of equiaxed grains; (b) grain with annealing twins (×494 magnification); (c) rough surface with α grains and annealing twins; and (d) rough surface with embedded inclusions (arrows)*

of equiaxed grains with annealing twins, as well as deformation slip bands, was also observed by LM and SEM at the P-section after chemically polishing the sheet's surface with phosphoric acid + nitric-acid + acetic acid ($H_3PO_4 \cdot HNO_3 \cdot CH_3COOH$) solution (Figs. 8a–8c and Fig. 9, respectively).

The EDS analysis of the as-retrieved surface (area of exposed metal grains, Figs. 7a–7b) showed a composition of 49.7–49.9 wt% Cu, 28.3–30.6 wt% Zn, 6.9–9.7 wt% C, 7.9–12.8 wt% O, 0.9 wt% S and 1.2 wt% Cl (average values shown in Table 3). The EDS analysis results of the sheet after polishing its surface (Fig. 9) revealed a composition of 52.1–65.3 wt% Cu, 14.2–24.5 wt% Zn, 11.0–28.0 wt% O, 0.9–4.5 wt% S and 0.7–1.5 wt% Cl (average values shown in Table 3).

The composition of the as-retrieved Cu-Zn alloy (before grinding), based on the SEM-EDS surface analysis (after eliminating elements other than Cu and Zn), was 61.8–63.8 wt% Cu and 36.2–38.2 wt% Zn, with a Cu/Zn ratio of 1.6–1.8. However, the composition of the chemically polished sheet (after eliminating other elements than Cu and Zn) was 69.1–78.6 wt% Cu and 21.4–30.6 wt% Zn, with Cu/Zn ratio of 2.3–3.7.
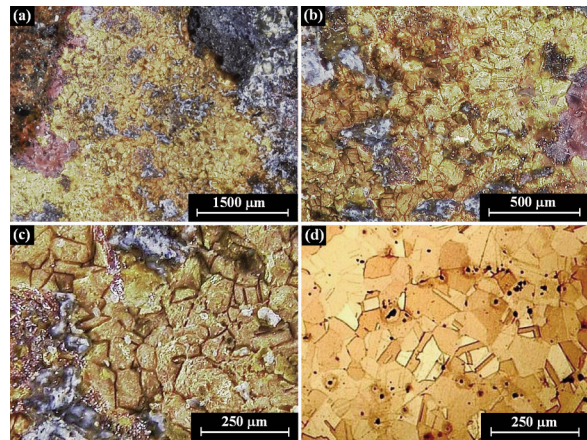


*Figure 8. LM images of the sheet (P-section): (a) general view of the surface (polished, multi-focal LM) with brown, red, and pink colours of oxides (left side of image), and grey and black colours of oxides (right side of image) and exposed metal (centre of image); (b) different oxides and metal grains (polished, multi-focal LM); (c) equiaxed α grains and annealing twins (polished, multi-focal LM); and (d) metallographic image of the equiaxed α grains, annealing twins and inclusions (ground, polished and etched sample, LM).*
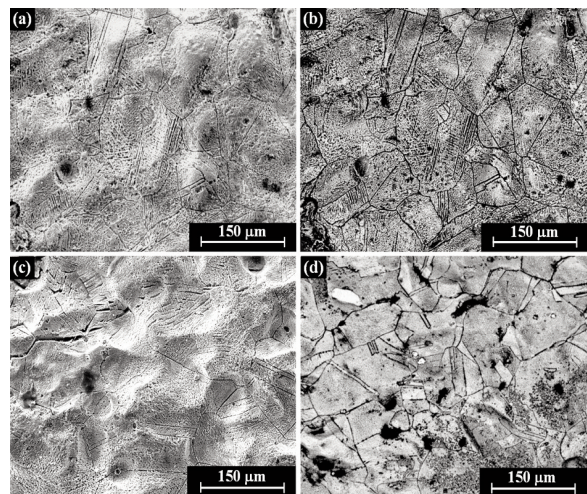


*Figure 9. SEM images of the sheet (P-section, polished): (a) equiaxed α grains and annealing twins (SE mode); (b) α grains, annealing twins and slip bands (BSE mode); (c) α grains, cracks, twins and slip bands (SE); and (d) equiaxed grains and annealing twins (BSE)*

### 3.2. Bulk metal characterization

VT of the bulk revealed it was well-preserved. The XRF analysis results of the sheet's base metal surface (average of eight areas measured from both sides of the sheet) after grinding indicated a composition of 64.7±0.7 wt% Cu, 34.4±0.4 wt% Zn, as well as the presence of Pb, Sn, Si, S and Al (P-section, Table 2).

*Table 3.* *SEM-EDS analysis results of the sheet's oxide surface as-retrieved and of the sheet's bulk after grinding*

| Sample | Composition weight percentage (wt%) | | | | | | |
|---|---|---|---|---|---|---|---|
| | **Cu** | **Zn** | **C** | **O** | **S** | **Na** | **Cl** |
| As-retrieved oxide rough surface | 30.5 | 23.7 | 12.7 | 25.5 | 0.7 | 6.5 | 0.4 |
| As-retrieved naturally etched surface of exposed grains (average of two measurements) | 49.7 | 29.5 | 8.3 | 10.4 | 0.9 | – | 1.2 |
| The polished surface (average of four measurements) | 59.1 | 20.4 | – | 16.9 | 2.5 | – | 1.1 |
| Bulk metal, metallographic sample after grinding the surface (average of five measurements) | 63.3 | 34.8 | – | 1.7 | 0.2 | – | – |

The transverse cross-section (T-CS) of a sample of the sheet was ground and a 1 mm thickness was removed in order to examine its bulk, which was found to be very well preserved. SEM-EDS analysis of the ground sample (T-CS, average of five measurements) indicated a composition of 63.3 wt% Cu, 34.8 wt% Zn, 1.7 wt% O and 0.2 wt% S (Table 3); and the composition (after eliminating elements other than Cu and Zn) was of 63.6–64.9 wt% Cu and 35.1–36.4 wt% Zn. Therefore, the Cu/Zn ratio of the ground T-CS of the sheet's bulk was 1.7–1.8.

S-OES destructive chemical analysis results of the bulk of the sheet revealed that it was made of α-brass, with composition of 65.0 wt% Cu, 34.4 wt% Zn and 0.6 wt% Pb. Microstructure of equiaxed grains containing inclusions and annealing twins was observed at the bulk of the metal by LM on both the metallographic T-CS and P-CS after etching of the surface with hydrochloric acid in ferric chloride solution (Fig. 8d), as expected from rolled and annealed sheet. The grain size (diameter) on both the T- and P-sections was 50–180 μm (Figs. 6–9).

### 4. Discussion

Sheathing the submerged part of the hulls of ships was an important development in the process of improving their durability, and different metals for sheathing and fastenings were tested [46, 47]. Therefore, using metallurgical methods (Table 1) to investigate such a sheet retrieved from a shipwreck increases our knowledge of manufacturing technologies of marine sheathing materials in Europe during the first half of the nineteenth century. Moreover, the results expand our knowledge of the corrosion processes of α-brass during a long burial period in marine environments.

From the perspective of archaeology, determination of the chemical composition and microstructure of the base metal provides significant information. Hence, it is important to determine whether the composition and microstructure of the surface are different than the bulk material of the

archaeological object [48]. Since the surface analysis of metals retrieved from marine environment may not be a good representative of the object's bulk (due to oxide layers and corrosion products), both the surface and the bulk of the brass sheet retrieved from the Akko Tower Wreck were examined by metallurgical analyses (Table 1). S-OES bulk analysis results revealed that the sheet was made of α-brass, with composition of 65.0 wt% Cu, 34.4 wt% Zn and 0.6 wt% Pb. Similar sheets were manufactured during the nineteenth century by hot rolling [14, 16, 49].

The lead might originate from the zinc ore, or perhaps it was deliberately added to improve the casting quality and the machinability of the alloy [11, 45]. The XRF and EDS analyses of the bulk of the sheet (Tables 2 and 3) are in good agreement with the S-OES analysis results. Such a brass alloy has excellent corrosion resistance combined with good mechanical properties, and was widely used in marine environments in the mid-nineteenth century [14, 16, 47,50–52]. Nevertheless, in some hostile environments brass can suffer from aggressive corrosion processes [36].

The XRF analysis results of the brass sheet surface after grinding with SiC papers revealed the presence of up to 0.8 wt% Si and up to 0.4 wt% Al. The XRF results of the as-retrieved sheet (oxide surface) also indicated the presence of 0.4±0.1 wt% Si and 0.1±0.1 wt% Al (Table 2). Since no silicon or aluminium was found in the S-OES bulk analysis and in the EDS analysis of the sheet after removal of the 1 mm layer, the presence of Si and Al (as well as other elements, such as P, S, Ca and Cl) is most likely related to reactions between soil elements and corrosion products [42–43, 46]. For example, the Al presence may be related to long term intergranular corrosion processes [53].

This good corrosion resistance of α-brass results from the formation of ZnO and complex passive $Cu_xO_y$ oxides on the surface of the metal [30, 42]. Copper oxide is an antibacterial compound, and doping Zn ions into the copper-oxide film increases the antibacterial activity of the metal [31, 54, 55]. Indeed, the toxic

nature of brass in sea water environments has been used over the last two hundred years as a protection mechanism for preventing attack by marine organisms and marine fouling on wooden vessels [56].

The corrosion products on the surface of the sheet had a composition of about ~50 wt% Cu and ~30 wt% Zn with C, O, S and Cl contaminants according to EDS analysis (before grinding). The colour differences on the surface of the sheet (Fig. 3) may be a result of the surface composition: blue is possibly copper hydroxide and chlorides (posnjakite); green is usually related to copper sulphates (atacamite, paratacamite, brochantite) and/or with basic copper chlorides; turquoise colour may be related to the presence of namuwite and/or to hydrous copper chlorosulphate (connellite); white is most likely related to zinc compounds, e.g. zinc oxide/hydroxide and zinc chloride; the gold-yellowish colour is attributed to $CuCl_2$ (tolbacite); pink may be attributed to zinc hydroxichloride; and the reddish colour is due to cuprite [11, 35–39]. The XRD results of the sheet's surface revealed presence of metallic brass as well as different oxides, including cuprite, namuwite, connellite and hydrated zinc chlorosulphate (Fig. 5).

S-OES, XRF and EDS analyses of the sheet's bulk indicated 34.2–36.4 wt% Zn. However, the EDS analysis of the sheet after chemically polishing its surface revealed 20.6–22.1 wt% Zn, 11.0–12.5 wt% O and 0.7–1.1 wt% Cl. This may have resulted from dezincification of the polished surface. The occurrence of copper and zinc minerals together suggests a complex relationship between $Cl^-$ and $SO_4^{2-}$ ions in the corrosion of brass in seawater. The dezincification of brass is one of the recognized forms of its corrosion [39, 42, 56]. When brass is immersed in seawater only zinc is dissolved; causing the formation of a surface layer enriched in copper, and generating defects in the crystalline structure. These defects promote zinc diffusion from the bulk alloy, and increase the copper's tendency to dissolve from the outer layer. The thickness of this layer becomes constant, zinc diffusion becomes steady-state, and its content at the alloy surface tends to zero. During long exposure underwater, the uniform dissolution of brass occurs, and zinc and copper pass into the surrounding medium in the same ratio as they are present in the alloy [57]. The constant Cu/Zn ratio determined in the brass sheet before and after grinding confirms this phenomenon, with ratios of 1.6–1.8 and 1.7–1.8, respectively. However, it should be noted that after chemically polishing the brass sheet, this Cu/Zn ratio was significantly increased to 2.3–3.7 as a result of the preferable zinc dissolution in applied acidic solution, and is evidence of dezincification.

The exposed as-retrieved brass microstructure, of equiaxed $\alpha$-grain and annealing twins, observed on the sheet's surface (Figs. 6 and 7) is most likely the result of intensive local etching of its surface in seawater due to specific defects (e.g. micro-cracks, stress), caused during the manufacture of the sheet. An example of such defects related to the manufacturing process of the sheet is the presence of grain boundaries and areas rich in deformation slip bands (Fig. 9). This makes brass surface electrochemically non-uniform in a corrosive environment. Corrosion cells at $\alpha$-brass surface are not very effective in a neutral medium, but in acidic solutions, their current increases significantly. That is why $\alpha$-brasses are etched non-uniformly in acidic media due to intensive dissolution of the intergranular space enriched in zinc [57]. Since the corrosion rate is dependent on various factors, such as temperature, pH, salinity and dissolved oxygen concentration of sea water, bio-activity, wave action, monsoon rain and settlement which are seasonally variable, the fluctuation of the surrounding environments, as well as storms or mechanical damage of the protective oxide coating, allow partial dissolution of the brass corrosion product or its peeling off the substrate, exposing the brass to renewed corrosion, resulting in native etching of the brass surface (Figs. 6 and 7).

The relatively uniform thickness of the sheet (average 0.85 mm), its general microstructure, and the presence of twinning defects, all indicate that it was manufactured by rolling and annealing. Such a sheet was fabricated from flat cast blanks. During the rolling process the material had to be annealed several times before the sheet reached the required thickness [16]. Similar rolled $\alpha$-brass sheets were used at the beginning of the nineteenth century for the manufacture of brass objects for marine use. For example, 158 brass cases were retrieved from the Akko 1 shipwreck, which was an Egyptian naval auxiliary brig of about 26 m long, built in the first third of the nineteenth century. The brass cases of Akko 1 had a uniform thickness of 0.5–0.55 mm. Based on their microstructure, including the presence of preferred oriented imperfections, these cases were produced of $\alpha$-brass rolled sheets [14, 16, 28, 29]. In another example from the nineteenth century Puerto Pirámides 1 shipwreck (Argentina), the rolled brass sheathing was 0.41±0.07 mm thick. However, the thickness of the sheet including the oxide layer was 0.9–1.2 mm. Both sides of the Puerto Pirámides 1 brass sheet were covered with dark black, green and turquoise corrosion products [46].

In the case of the Akko Tower shipwreck, the high zinc concentrations in the alloy indicate that the metal used for manufacturing the sheet was most likely new and not recycled. The nominal thickness of the brass sheet was approximately 0.85 mm, which corresponds to British 21 (0.81 mm) or 20 (0.89 mm) BWG. This may indicate that it was produced according to British standards.

## 5. Conclusions

The brass sheet retrieved from the Akko Tower Wreck was most likely manufactured during the first half of the nineteenth century, according to British standards. Based on its characteristics, such as thickness and corrosion resistance of α-brass, it provides additional evidence for the use of brass sheathing during this period to protect the hull against marine organisms, and to improve the sailing qualities of the ship. The as-retrieved surface of the sheet exhibits a unique example of a surface after almost two hundred years under the sea, resulting from local etching of the sheet due to specific defects at the microscopic level, such as grain boundaries and slip bands, indicating a microstructure of annealed α-brass, similar to that of the sheet's bulk. The results provide further information about the Akko Tower shipwreck; and expand our knowledge regarding the corrosion processes and preservation of brass during a long burial period in marine environments.

## Acknowledgements

## References

[1] E.D. Clarke, Travels in Various Countries of Europe, Asia and Africa, Part the second, Greece, Egypt and the Holy Land, Section the first Vol. IV, T. Caddell and W. Davies, London (1817), pp. 88–89.

[2] R.C. Alderson, Notes on Acre and Some of the Coast Defences in Syria, Papers on Subjects Connected with the Duties of the Corps of Royal Engineers VI 28, John Weale, London (1843), pp. 39–48.

[3] C. La Jonquière, L'expédition d'Egypte, 1798–1801, Vol. IV, H. Charles-Lavauzelle, Paris (1900).

[4] R.C. Anderson, Naval Wars in the Levant 1559–1853, University Press of Liverpool, Liverpool (1952), pp. 372–373, 561–564.

[5] A. Rustum, Notes on Akka and its Defences under Ibrahim Pasha, Archaeological Congress of Syria and Palestine, American University of Beirut, Beirut (1926).

[6] T.H. Molyneux, J. Royal Geograph. Soc. London 18 (1948) 104–130.

[7] A. Flinder, E. Linder, E.T. Hall, The survey of the ancient harbour of Akko 1964–1966, in: M. Heltzer, A. Segal, D. Kaufman (Editors), Studies in the Archaeology and History of Ancient Israel, in Honour of Moshe Dothan, Haifa University Press, Haifa (1992), pp. 199–225.

[8] A. Raban, A shipwreck from Napoleon's siege of Akko (1799), in: M. Yedaya (Editor), The Western Galilee Antiquities (in Hebrew), Tel Aviv (1986), pp. 195–208.

[9] J.R. Steffy, The Napoleonic Wreck: A Workshop in Ship Construction, Unpublished Report, Institute of Nautical Archaeology, Texas A&M University, College Station, Texas (1983).

[10] C. Cvikel, Intern. J. Naut. Archaeo. 54(2) (2016) 406–422.

[11] M. Cohen, D. Ashkenazi, Y. Kahanov, A. Stern, S. Klein, D. Cvikel, Metallogr. Microstruct. Anal. 4(3) (2015) 188–206.

[12] A. Hauptmann, R. Maddin, M. Prange, Bull. Amer. Sch. Orient. Res. 328 (2002) 1–30.

[13] M. Eliyahu, O. Barkai, Y. Goren, E. Eliaz, Y. Kahanov, D. Ashkenazi, J. Archaeo. Sci. 38 (2011) 233–245.

[14] D. Ashkenazi, D. Cvikel, N. Iddan, E. Mentovich, Y. Kahanov, M. Levinshtein, J. Archaeo. Sci. 38(9) (2011) 2410–2419.

[15] D. Cvikel, D. Ashkenazi, A. Stern, Y. Kahanov, Mater. Character. 83 (2013) 198–211.

[16] D. Ashkenazi, D. Cvikel, A. Stern, S. Klein, Y. Kahanov, Mater. Character. 92 (2014) 49–63.

[17] Y. Kahanov, D. Ashkenazi, D. Cvikel, S. Klein, R. Navri, A. Stern, J. Archaeo. Sci. Rep. 2 (2015) 321–332.

[18] D. Cvikel, T. Ben-Artzi, D. Ashkenazi, N. Iddan, A. Stern, Y. Kahanov, Archaeometry 58(3) (2016) 427–440.

[19] D. Cvikel, D. Ashkenazi, Metallogr. Microstruct. Anal. 5(1) (2016) 16–27.

[20] G.F. Van der Voort (Ed.), Metallography: An Introduction, Metallography and Microstructures, ASM Handbook vol. 9, ASM International, OH (2004), pp. 3–20.

[21] F.A. Paneth, Geochim. Cosmochim. Acta. 18(3-4) (1960) 176–182.

[22] R.L. Folk, Henry Clifton Sorby (1826–1908), J. Geolog. Edu. 3(2) (1965) 43–47.

[23] N.D. Greene, G.A. Teterin, Corros. Sci. 12(1) (1972) 57–63.

[24] J.R. Vilella, Metallographic Technique for Steel, Metals Park, Cleveland: American Society for Metals, OH (1938), pp. 26–52.

[25] D. Cvikel, E.D. Mentovich, D. Ashkenazi, Y. Kahanova, J. Min. Metall. Sect. B-Metall. 49(1) (2013) 107–119.

[26] A. Aronson, D. Ashkenazi, O. Barkai, Y. Kahanov, Mater. Character. 78 (2013) 108–120.

[27] D. Ashkenazi, D. Cvikel, N. Iddan, E. Mentovich, Y. Kahanov, M. Levinshtein, J. Archaeo. Sci. 38(9) (2011) 2410–2419.

[28] J. Bezecný, A. Dubec, Procedia Eng. 136 (2016) 137–142.

[29] W. Ozgowicz, E. Kalinowska-Ozgowicz, B.

Grzegorczyk, J. Achievem. Mater. Manuf. Eng. 40(1) (2010) 15–24.

[30] D. Cvikel, D. Ashkenazi, A. Inberg, I. Shteiman, N. Iddan, Y. Kahanov, Metallogr. Microstruct. Anal. 6(1) (2017) 12–21.

[31] D. Ashkenazi, A. Inberg, D. Langgut, N. Hendler, D. Cvikel, Corros. Sci. 110 (2016), 228–241.

[32] M.I. Barrena, J.M. Gomez de Salazar, A. Soria, Mater. Let. 62(3) (2008) 3944–3946.

[33] O. Papadopoulou, J. Novakovic, P. Vassiliou, E. Filippaki, Y. Bassiakos, Appl. Phys. A 113(4) (2013) 981–988.

[34] A. Srivastava, R. Balasubramaniam, Mater. Sci. 26 (2003) 593–600.

[35] G.A. El-Mahdy, J. App. Electrochem 35(3) (2005) 347–353.

[36] H. Fan, S. Li, Z. Zhao, H. Wang, Z. Shi, L. Zhang, Corros. Sci. 53(12) (2011) 4273–4281.

[37] M.C. Bastos, M.H. Mendonça, M.M.M. Neto, M.M.G.S. Rocha, L. Proença, I.T.E. Fonseca, J. Appl. Electro. 38 (2008) 627–635.

[38] A. Mathiazhan, R. Joseph, K.P. Narayanan, P. Seralathan, India J. Marine Sci. Tech. 18(5) (2010) 719–722.

[39] C.I.S. Santos, M.H. Mendonca, I.T.E. Fonseca, J. Appl. Electrochem. 36(12) (2006) 1353–1359.

[40] P. Stoffyn-Egli, D.E. Buckley, J.A. Clyburne, App. Geochemis. 13(5) (1998) 643–650.

[41] A. Doménech-Carbó, M. Doménech-Carbó, M.I. Martínez-Lázaro, Microchim. Acta 162(3) (2008) 351–359

[42] O. Papadopoulou, P. Vassiliou, S. Grassini, E. Angelini, V. Gouda, Mater. Corros. 160. 67(2) (2006) 160–169.

[43] M. Wadsak, I. Constantinides, G. Vittiglio, A. Adriaens, K. Janssens, M. Schreiner, F.C. Adams, P. Brunella, M. Wuttmann, Microchim. Acta 133(1) (2000) 159–164.

[44] A. N. Shugar, Portable X-ray fluorescence and archaeology: Limitations of the instrument and suggested methods to achieve desired results, in: R.A. Armitage and J.H. Burton (Eds.), Archaeological Chemistry VIII, American Chemical Society, Washington DC (2013), pp. 173–193.

[45] C. Martini, C. Chiavari, F. Ospitali, F. Grazzi, A. Scherillo, C. Soffritti, G.L. Garagnani, Mater. Chem. Phys. 142 (2013) 229–237.

[46] H.M. De Rosa, N.C. Ciarlo, M. Pichipil, A. Castelli, Proc. Mater. Sci. 9 (2015) 177–186.

[47] J.M. Bingeman, J.P. Bethell, P. Goodwin, A.T. Mack, Inter. J. Naut. Archaeo. 29(2) (2000) 218–229.

[48] D. Ashkenazi, H. Gitler, A. Stern, O. Tal, Sci. Rep. 7 (2017) 1–14.

[49] I.D. MacLeod, Corros. Prevent. (2016) 1–10.

[50] P. Qiu, C. Leygraf, Appl. Surf. Sci. 258 (2011) 1235–1241.

[51] T.S. Rao, K.V.K. Nair, Corros. Sci. 40(11) (1998) 1821–1836.

[52] M. Staniforth, The introduction and use of copper sheathing-A history, Newsletter Australian Instit. Maritime Archaeo. 9 (1985) 21–48.

[53] G.M. Ingo, T. De Caro, C. Riccucci, E. Angelini, S. Grassini, S. Balbi, P. Bernardini, D. Salvi, L. Bousselmi, A. Cilingiroglu, M. Gener, Appl. Phys. A 83(4) (2006) 513–520.

[54] W. Jiang, H. Mashayekhi, B. Xing, Environm. Pollu. 157(5) (2009) 1619–1625.

[55] N. Jones, B. Ray, K.T. Ranjit, A.C. Manna, FEMS, Microbio. Lett. 279(1) (2008) 71–76.

[56] I.D. MacLeod, Intern. J. Naut. Archaeo. 11(4) (1982) 267–275.

[57] I.K. Marshakov, Protec. Metals. 41(3) (2005) 205–210.

# ANALIZA PRIRODNO NAGRIZENE POVRŠINE MESINGANE OPLATE OLUPINE BRODA IZ DEVETNAESTOG VEKA

**D. Ashkenazi [a*], A. Inberg [b], and D. Cvikel [c]**

[a] Mašinski fakultet, Univerzitet u Tel Avivu, Izrael
[b] Elektrotehnički fakultet, Univerzitet u Tel Avivu, Izrael
[c] Pomorski institut ‚Leon Recanati' i Odsek za pomorske civilizacije, Univerzitet u Haifi, Izrael

*Apstrakt*

*Olupina broda kod Akra tvrđave je očito ostatak dvadeset i pet metara dugačkog trgovačkog jedrenjaka sa dve katarke iz prve polovine devetnaestog veka. Tokom podvodnih iskopavanja 2015. godine, parče mesingane ploče je spaseno iz olupine broda, i metalurškim analizama su ispitane i površina i masa ploče. Ispitivanja su otkrila jedinstveni primer prirodnog nagrizanja koje je trajalo gotovo dvesta godina ispod površine mora. Površina ploče bila je prekrivena različitim oksidima bakra i cinka, što je utvrđeno XRD analizom. Posmatranje prirodno nagrizene površine multifokalnim svetlosnim mikroskopom, kao i SEM-EDS analiza, ukazali su na mikrostrukturu odžarenog α-mesinga, sličnu mikrostrukturi mase ploče. S-OES hemijska analiza mase otkrila je hemijski sastav od 65.0 wt% Cu, 34.4 wt% Zn and 0.6 wt% Pb. Sudeći po debljini i očuvanosti ploče, pretpostavlja se da je korišćena kao oplata koja je štitila trup broda od morskih organizama, kao i da poboljša kvalitet jedrenja broda. Ovi rezultati daju nam dodatne informacije o olupini broda, i proširuju naše znanje o procesima korozije i očuvanju mesinga tokom dugog perioda ispod površine mora.*

*Ključne reči: Olupina broda kod Akra tvrđave; Mesingana ploča; Korozija; Metalografija; Metalurgija; Prirodno nagrizena površina*